Liquid Crystals
Publication details, including instructions for authors and subscription information:
http://www.informaworld.com/smpp/title~content=t713926090

Dynamics of viscous fingers in Hele-Shaw cells of liquid crystals Theory and experiment

L. Lam[a]; H. C. Morris[b]; R. F. Shao[c]; S. L. Yang[c]; Z. C. Liang[c]; S. Zheng[c]; H. Liu[cd]
[a] Department of Physics, San Jose State University, San Jose, California, U.S.A. [b] Department of Mathematics and Computer Science, San Jose State University, San Jose, California, U.S.A. [c] Liquid Crystal Division, Department of Physics, Nanjing Normal University, Nanjing, China [d] Theoretical Physics Group, Cavendish Laboratory, Cambridge University, England

To cite this Article Lam, L. , Morris, H. C. , Shao, R. F. , Yang, S. L. , Liang, Z. C. , Zheng, S. and Liu, H.(1989) 'Dynamics of viscous fingers in Hele-Shaw cells of liquid crystals Theory and experiment', Liquid Crystals, 5: 6, 1813 — 1826
To link to this Article: DOI: 10.1080/02678298908045690
URL: http://dx.doi.org/10.1080/02678298908045690

LIQUID CRYSTALS, 1989, VOL. 5, NO. 6, 1813–1826

Dynamics of viscous fingers in Hele–Shaw cells of liquid crystals Theory and experiment

by L. LAM†, H. C. MORRIS‡, R. F. SHAO§, S. L. YANG§, Z. C. LIANG§, S. ZHENG§ and H. LIU§¶

† Department of Physics, San Jose State University, San Jose, California 95192, U.S.A.

‡ Department of Mathematics and Computer Science, San Jose State University, San Jose, California 95192, U.S.A.

§ Liquid Crystal Division, Department of Physics, Nanjing Normal University, Nanjing, China

¶ Theoretical Physics Group, Cavendish Laboratory, Cambridge University, England

The theoretical and experimental developments in the interfacial dynamics and the formation of viscous fingering patterns in Hele–Shaw cells of liquid crystal-air systems are summarized and discussed. These include radial and linear cells with or without grooves engraved on the cell plates. Instabilities of fingers, the role of intrinsic and extrinsic anisotropies, etc., are emphasized. In a linear cell, when the injected air is kept at constant pressure, a whole sequence of successive instabilities of fingers (hump, tip-splitting, sidewrinkling, sidebranching and DLA-like structure) is observed in a single run of the experiment. In our theory, the equations of motion of nematic flows in Hele–Shaw cells are derived from the Ericksen–Leslie equations. In the linear approximation, the equations resemble those of isotropic liquids with the presence of effective viscosities and anisotropic surface tension. Experimental observations are interpreted with the introduction of an effective control parameter which may be time dependent. Special features of viscous fingers in liquid crystals in contrast to those in isotropic liquids, such as asymmetric dendritics, displacement of the finger from the central axis of the linear cell, and reentrant sequence of patterns, are pointed out. Plausible explanations of these phenomena are given. In this newly developed field, a large number of interesting problems remain to be solved.

1. Introduction

The formation of viscous fingering patterns [1, 2] is one of many such problems in systems far from equilibrium, such as diffusion-limited aggregation (DLA) [3], electrodeposition [4] and directional solidification [5]. These patterns are governed by the interplay of anisotropy, fluctuations (noise) and the driving force in each case [6]. The development in last few years shows the emergence of a unifying principle of 'microscopic solvability' underlying the pattern formation in these diverse systems [7].

Viscous fingers appear as interfacial patterns when a viscous fluid is displaced by a less viscous fluid [8] in a Hele–Shaw cell, i.e. two plates with very small separation b. In the original experiment of Saffman and Taylor [8], a linear cell was used and a steady single finger appeared with λ approximately equal to 1/2. Here λ is the ratio of the finger width to the cell width w. Subsequently, a radial Hele–Shaw cell was used by Paterson [9].

0267–8292/89 $3.00

There are three major areas in the study of viscous fingers using isotropic liquids:

(i) Formation of fingers. Experimentally a single steady finger of well defined shape is observed. How this can be understood theoretically is a typical pattern-selection problem. Furthermore, properties of the unstable interface before the emergence of a single finger [1, 2], or fingers in the case of a radial cell [10], are well studied.

(ii) Instabilities of fingers. This problem has been investigated theoretically [7, 11–14] and experimentally [15, 16]. Noise is found to be important in producing instabilities such as the symmetric nonoscillatory mode, hump, tip-wobbling, sidebranching and tip-splitting, even though the finger is linearly stable. In linear cells only tip-splitting [15, 16] and hump [16] are observed.

(iii) The role of anisotropy. Anisotropy is demonstrated experimentally [17 (a)] in a radial cell as a necessary condition for dendritics with stable tips to form. With anisotropic surface tension the finger in a linear cell is predicted [17 (b)] to assume a family of possible widths.

In [17 (a)] *extrinsic* anisotropy (produced by engraving a triangular or square grid on the cell plate) is used. Since liquid crystals are *intrinsically* anisotropic they become the natural media to be used in Hele–Shaw cells to study anisotropic and other effects. Experimental works in this regard include those of Buka *et al.* [18–20], Shao, Liu and Lam [21], Zheng *et al.* [22], and Yang *et al.* [23]. Theoretical study specific to liquid crystal flows in Hele–Shaw cells was given by Lam [24].

Here, theoretical [24] and experimental [18–23] developments mentioned above, together with some new results, will be summarized and discussed. Special attention will be given to non-steady situations. The presentation is unavoidably brief due to the limited length of this paper. More details can be found in [24]. A large number of unsolved problems are noted.

2. Theory

From the Ericksen–Leslie theory, the flow of incompressible nematics in a Hele–Shaw cell is found to be described by [24]

$$\varrho v_{i,t} + p_{,i} = [-Kn_{j,i}n_{j,z} + \sigma'_{iz}]_{,z}, \quad i = x, y, z \tag{1}$$

and

$$-\gamma_1 \begin{pmatrix} n_{x,t} \\ n_{y,t} \\ n_{z,t} \end{pmatrix} + \begin{pmatrix} -\alpha_2 n_z & 0 & n_x \\ 0 & -\alpha_2 n_z & n_y \\ -\alpha_3 n_x & -\alpha_3 n_y & n_z \end{pmatrix} \begin{pmatrix} v_{x,z} \\ v_{y,z} \\ \alpha \end{pmatrix} = -K \begin{pmatrix} n_{x,zz} \\ n_{y,zz} \\ n_{z,zz} \end{pmatrix}, \tag{2}$$

where $\hat{z}$ is the normal of the cell, $(\ldots)_{,z} \equiv \partial(\ldots)/\partial z$, etc., and the one-elastic constant approximation is assumed. All quantities are functions of x, y, z and t, and $v_z = 0$. α is a Lagrangian multiplier due to $\mathbf{n}^2 = 1$. $\mathbf{v}$ and $\mathbf{n}$ are velocity and director of the molecule, respectively, and p is the pressure. Here,

$$\begin{aligned} \sigma'_{xz} &= v_{x,z}[\alpha_1 n_x^2 n_z^2 + \tfrac{1}{2}(\alpha_3 + \alpha_6)n_x^2 + \tfrac{1}{2}(\alpha_5 - \alpha_6)n_z^2 + \tfrac{1}{2}\alpha_4] \\ &\quad + v_{y,z}[\alpha_1 n_z^2 + \tfrac{1}{2}(\alpha_3 + \alpha_6)]n_x n_y + \alpha_2 n_z n_{x,t} + \alpha_3 n_x n_{z,t}, \end{aligned} \tag{3}$$

$$\begin{aligned} \sigma'_{zz} &= v_{x,z}[\alpha_1 n_z^2 + \tfrac{1}{2}(\alpha_2 + \alpha_3 + \alpha_5 + \alpha_6)]n_x n_z \\ &\quad + v_{y,z}[\alpha_1 n_z^2 + \tfrac{1}{2}(\alpha_2 + \alpha_3 + \alpha_5 + \alpha_6)]n_y n_z + (\alpha_2 + \alpha_3)n_z n_{z,t}, \end{aligned} \tag{4}$$

σ'_{yz} is given by (3) with the interchange of x and y. In (2), using $n_i n_{i,j} = 0$, $n_{z,zz}$ can be replaced by

$$n_{z,zz} = -\left(\frac{n_x}{n_z} n_{x,z} + \frac{n_y}{n_z} n_{y,z}\right)_{,z}. \tag{5}$$

In the steady or quasisteady case, equation (2) can be solved to give

$$Dv_{x,z} = K\,[n_{x,zz}(\alpha_2 n_z^2 - \alpha_3 n_y^2) + n_{y,zz}\,(\alpha_3 n_x n_y) + n_{z,zz}\,(-\alpha_2 n_x n_z)]. \tag{6}$$

Similarly, $v_{y,z}$ is given by (6) with the interchange of x and y. The determinant D is given by

$$D = -\alpha_2 n_z\,[\alpha_3 - (\alpha_2 + \alpha_3) n_z^2]. \tag{7}$$

In principle, $v_{x,z}$ and $v_{y,z}$ from (6) can be put into (3) and (4), and then in (1), resulting in an equation for $\mathbf{n}$ and p. After the solution for $\mathbf{n}$ is obtained equation (6) will give the solution for $\mathbf{v}$. This procedure is straightforward but rather complicated.

For simplicity, as a first approximation, we keep only first-order terms in (3), (4) and (6). This corresponds to a linearization of all the equations.

Case 1. Homeotropic cell

For a homeotropic cell, $n_z \simeq 1$, n_x, n_y are small quantities. We have

$$p_{,i} = \mu_z v_{i,zz}, \quad i = x, y, \tag{8}$$

$$p_{,z} = 0 \tag{9}$$

and

$$n_{i,zz} = (\alpha_2/K) v_{i,z}, \quad i = x, y, \tag{10}$$

where

$$\mu_z \equiv \tfrac{1}{2}(\alpha_4 + \alpha_5 - \alpha_2). \tag{11}$$

Case 2. Planar-x cell

We assume molecules are aligned in x direction at the plates, and $n_x \simeq 1$, n_y, n_z small. We then have

$$p_{,x} = \mu_x v_{x,zz}, \tag{12}$$

$$p_{,y} = \mu_y v_{y,zz}, \tag{13}$$

$$p_{,z} = 0, \tag{14}$$

where

$$\mu_x \equiv \tfrac{1}{2}(\alpha_3 + \alpha_4 + \alpha_6), \quad \mu_y \equiv \tfrac{1}{2}\alpha_4. \tag{15}$$

To this order of approximation, equation (6) is identically satisfied.

Case 3. Planar-y cell

For molecules parallel to y direction at the plates, $n_y \simeq 1$, n_x, n_z are small. We then obtain equations identical to (12)–(14), and with x, y interchanged in (15). For a linear cell case 3 is different from case 2, assuming the long axis of the cell to be the x axis, say. The two cases are identical in an infinite radial cell.

Case 4. Untreated cell

For a cell with untreated surfaces, let $n_i n_j \simeq \langle n_i n_j \rangle = \frac{1}{3}\delta_{ij}$, $i, j = x, y, z$. We then have

$$p_{,i} = \mu_0 v_{i,zz}, \quad i = x, y, \tag{16}$$

$$p_{,z} = 0, \tag{17}$$

where

$$\mu_0 \equiv \tfrac{1}{2}\alpha_4 + \tfrac{1}{9}\alpha_1 + \tfrac{1}{6}(\alpha_3 + \alpha_6 + \alpha_5 - \alpha_2). \tag{18}$$

In cases 2 and 3, we may rescale x and y to make the effective viscosities in (12) and (13) to be identical to each other. The four cases considered then have the same equations as in (8) and (9), but with different μ_z there. Equations (8) and (9) are the same as that for an isotropic liquid [25], resulting in

$$\mathbf{V}(x, y) = -k\nabla p(x, y), \tag{19}$$

where $\mathbf{V}$ is the z-averaged $\mathbf{v}$, and $k \equiv b^2/12\mu$.

At this level, the major difference between anisotropic and isotropic liquids lies in the boundary conditions. For liquid crystals the pressure drop across the interface is given by

$$\Delta p = \sigma(\mathbf{n}_0)/R, \tag{20}$$

where the surface tension σ is a function of $\mathbf{n}_0$, $\mathbf{n}$ at the interface, and R is the radius of curvature of the interface in the plane of the cell. The fact that σ is indeed anisotropic has been shown theoretically [26] and experimentally [27].

For isotropic liquids, the wetting of the more viscous fluid on the plates gives a modified Δp [28],

$$\Delta p = \frac{\pi}{4}\frac{\sigma}{R} + \frac{2\sigma}{b}\left[1 + 3.80\left(\frac{\mu V_n}{\sigma}\right)^{2/3}\right], \tag{21}$$

where V_n is the normal velocity of the interface. Equation (21) will certainly be modified for liquid crystals. Its use for nematic-air interface [19, 20] may not be justified.

For the sake of discussion, in most cases of application one may adopt the results of (8)–(21) as far as qualitative results are concerned. The system is then treated as isotropic liquids with appropriate effective viscosities and σ in (20) and (21) as some averaged surface tension.

3. Experiments and discussion

In all experiments [8–10, 15–23] the less viscous fluid (air, say) is injected either with constant flux or at constant pressure. For a linear cell, the former method [16] corresponds to $U = \text{const}$ where U is V at the far end of the cell from which the more viscous fluid flows out. This is also the assumption used in all theoretical studies [8, 11–14]. In this case, the problem has a single dimensionless control parameter

$$\frac{1}{B} = 12\frac{\mu U}{\sigma}\left(\frac{w}{b}\right)^2, \tag{22}$$

which is constant throughout a single run of the experiment. Here the unit of length is w, μ the viscosity of the displaced fluid, and the air is assumed to have zero viscosity.

With the latter method [21, 23], injection at constant pressure, $1/B$ changes with time. If quasisteady state is assumed for every moment the finger advances one may use the instantaneous U in (22) and obtain an effective control parameter which is time dependent.

For a radial cell, one may use b as the unit of length and the control parameter of (22) is replaced by $1/C \equiv 12\mu U/\sigma$, which is time dependent for injection at constant pressure [17, 19, 20, 22].

Since instabilities and the resulting shapes of viscous fingers in a linear cell depend sensitively on $1/B$ [12, 14], one can expect the same to be true in a radial cell as $1/C$ changes. In other words, for air injected at constant pressure in a radial cell one should observe successive instabilities of the patterns in a single run (similar to the case in a linear cell [23]). In practice, this usually does not happen since the finite size of the cell (e.g. 6 cm in radius [20]) limits the change of $1/C$ to a small range.

3.1. *Radial cell without grooves*

In the radial cell experiments of Buka, Kertesz and Vicsek [18] using nematic mixtures, dendritic patterns were indeed observed. This confirms that intrinsic anisotropy in nematics has the same effect as extrinsic anisotropy [17 (a)] in stabilizing the tips *and* producing dendritics. (Note that extrinsic uniaxial anisotropy produces stable tips with only unpronounced sidebranches [29]. See figure 2 below.) Furthermore, a reentrant sequence of tip-splitting, dendritic, tip-splitting as a function of the flux of injected air is reported [18]. The mechanism of this phenomena is not yet clear. It is also noted [18] that surface treatment of the cell produced no appreciable effects. This may be understood from our linearized theory in §2, viz., the different surface treatments are expected to give quantitatively but not qualitatively different results.

Similar reentrant sequence of patterns in nematic 8CB (in untreated cell) as a function of temperature was observed [19, 20]. We note that the effective μ's in (11), (15), (18) and (21), and σ in (20) and (21) are all temperature dependent. Reentrant phenomena will result naturally from a non-monotonic curve of effective $1/C$ vs temperature. In [20] dense-branching patterns are found in the isotropic and smectic A phases of 8CB.

3.2. *Radial cell with concentric circular grooves*

A radial cell with concentric circular grooves on the inner surface of the lower square glass plate was constructed. The grooves have depth 0.3 mm, width 0.45 mm and edge to edge separation of 1 mm. There are 32 concentric grooves on the plate. The glass plates are cleaned but otherwise untreated. Nematic MBBA dyed red at 23°C are put inside the cell. Spacers of thickness b are put at the four corners of the cell. The cell is then clamped at the corners. The edges of the cell is opened to air at atmospheric pressure p_0. Air at constant pressure, $p_0 + p$, is injected through a small hole of diameter 1.5 mm at the centre of the upper plate.

In the thick cell, tip-splitting fingers and fingers with asymmetric sidebranching coexist with simple fingers (figure 1(a)). The pattern is similar to the dense-branching ones [10, 20] in the overall appearance. In the thin cell, the low p case (figure 1 (b)) has three branches and the high p case (figure 1 (c)) has more branches. In the latter, the trunk of the finger is smaller in width compared to that in the thick cell (with same p), and there are tip-splittings with the splitted two branches growing equally strong.

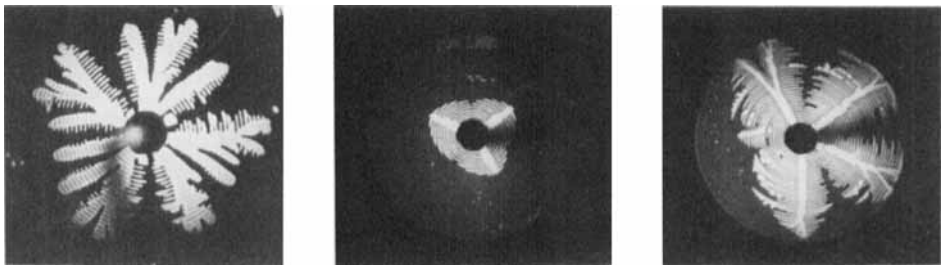

(*a*) (*b*) (*c*)

Figure 1. Patterns in radial cell of nematic MBBA with concentric circular grooves. (*a*) $b = 0{\cdot}12$ mm, $p = 5$ cm Hg. (*b*) $b = 0{\cdot}055$ mm, $p = 3$ cm Hg. (*c*) $b = 0{\cdot}055$ mm, $p = 5$ cm Hg. The few small bubbles are leftovers before air is injected at the centre.

Patterns like those in figures 1 (*b*) and (*c*) have not been seen before in either isotropic or anisotropic liquids.

3.3. *Radial cell with parallel grooves*

To further study the interplay between intrinsic and extrinsic anisotropies a radial cell with parallel grooves on the inner surface of the lower plate is used by Zheng *et al.* [22]. The grooves are 0·15 mm in depth, 0·15 mm in width, with edge-to-edge separation of 0·3 mm. The experimental procedure is similar to that in §3.2.

In the thin cell, $b = 0{\cdot}07$ mm, temperature $T = 34$°C, and p is varied from 0·5 to 4·5 cm Hg. A typical result is shown in figure 2 (*a*). Two dendritic fingers with rather sharp tips appear in the direction of the grooves. The left one is not identical to the right one. Side branches appear in the lower vertical finger. All these features are absent in the isotropic liquid-air system (figure 2 (*b*)). As p is varied,

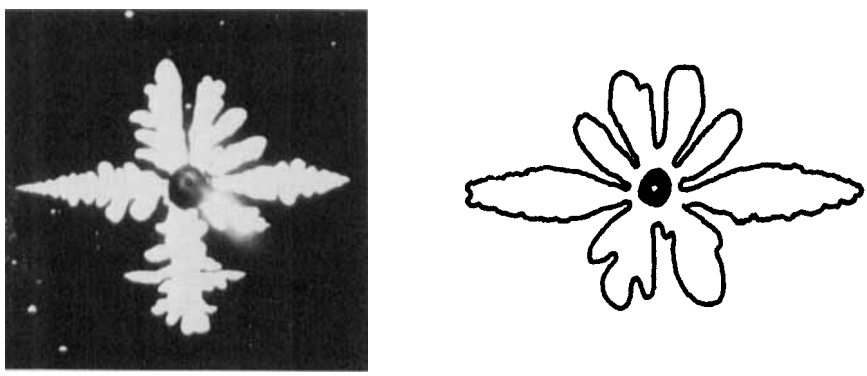

(*a*) (*b*)

Figure 2. Patterns in thin radial cell with parallel grooves. The direction of grooves is left–right in the diagram (same in figure 3). (*a*) Nematic MBBA–air system. $b = 0{\cdot}07$ mm, $p = 2{\cdot}5$ cm Hg. (*b*) Isotropic liquid–air system (adopted from [29]). Much more pronounced sidebranches appear in (*a*) than in (*b*). Two dendritic branches appear in (*a*), in contrast to the many and single dendritic branch in radial and linear cells, respectively.

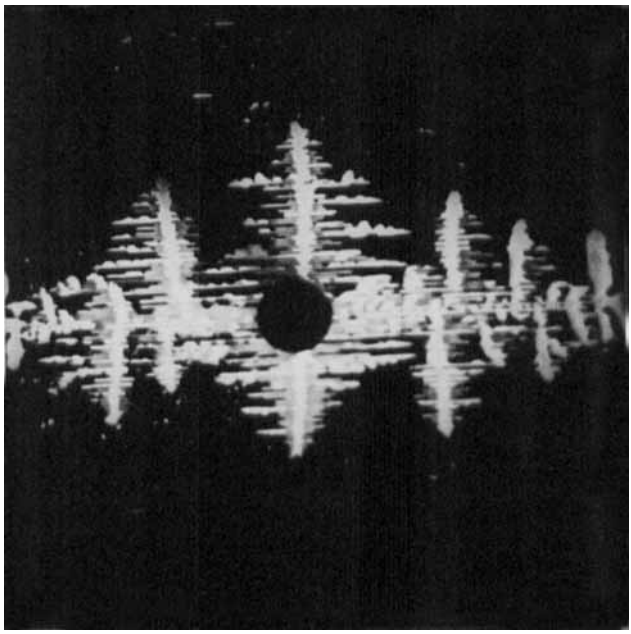

Figure 3. Patterns in thick radial cell of nematic MBBA with parallel grooves. $b = 0{\cdot}12$ mm, $p = 4$ cm Hg.

the sequence of patterns observed in this cell [22] differs from that reported in isotropic liquids [29].

In the thick cell, $b = 0{\cdot}12$ mm and $T = 32°C$. At $p = 4$ cm Hg, sidebranched fingers perpendicular to the grooves grow from the center *and* also from different points along the horizontal axis (figure 3). This interesting result is quite unexpected.

3.4. *Intermediate cell*

In radial cells, there are always more than one finger. In a linear cell, even though a single finger is obtained, the side-wall effect is dominant. (We are considering here cases without local external perturbations. Otherwise, a fast-growing finger with a double at the tip can come out from the several fingers in a radial cell [30] in which isotropic liquid is used.) To generate a single finger without much interference from the side walls, a square cell with cleaned but untreated glass plates of size $13 \times 13 \times 0{\cdot}5$ cm^3 each was used by Shao, Liu and Lam [21]. Spacers of width 5 mm and thickness 1·5 mm were put at three edges between the plates. The middle spacer was cut in the middle into two parts leaving a hole of $1{\cdot}5 \times 1{\cdot}5$ mm^2 in cross section. Air at constant pressure ($p_0 + p$) was injected through this hole into the cell. A sequence of photographs were taken for each p [21]. Single fingers were formed. Some results are presented in figure 4.

When nematic MBBA is used as the displaced fluid, for $p < 3$ cm Hg, the interface is almost a circle which grows to a radius of approximately 1 cm and stops expanding. For $p > 3$ cm Hg, the initially uncharacteristic interface is unstable and a pattern of multiple fingers is formed. The locations at which the fingers are formed are unpredictable. Some fingers grow faster than others (figure 4 (*b*)). For $p > 15$ cm Hg, the pattern is more like a piece of leaf, resulting from a series of tip-splitting bifurcations

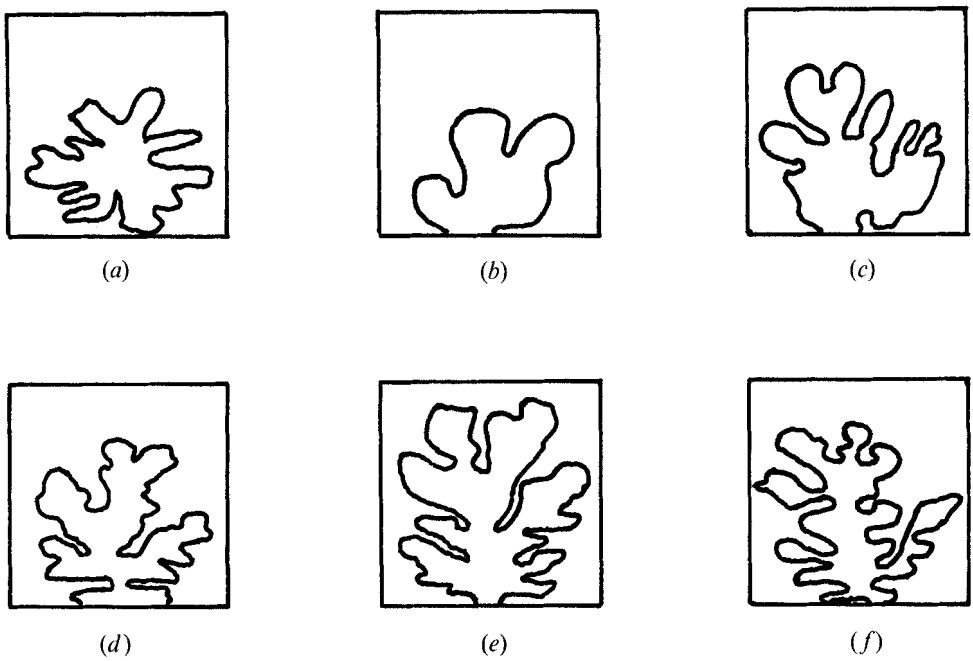

Figure 4. Viscous fingers in square cell with air injected through a hole in the middle of the lower edge. $T = 20°C$, $b = 1{\cdot}5$ mm. (*a*) Isotropic liquid (glycerin) displaced by air, $p = 35$ cm Hg. (*b*)-(*f*) Nematic MBBA displaced by air. (*b*) $p = 10$ cm Hg. (*c*) $p = 15$ cm Hg. (*d*) $p = 20$ cm Hg. (*e*) $p = 25$ cm Hg. (*f*) $p = 30$ cm Hg.

(figure 4 (*e*)). As shown in figures 4 (*b*)–(*f*), as p increases, the number of sidebranches increases and the width of the branch decreases. In comparison, when MBBA is replaced by glycerin, an isotropic liquid, the pattern is less leaf-like (figure 4 (*a*)).

In contrast to those in a radial cell [18], the patterns observed here are more asymmetric.

3.5. *Linear cell*

A linear cell similar to the one used by Saffman and Taylor [8] was constructed by Yang *et al.* [23]. The glass plate is $380 \times 60 \times 2\,\text{mm}^3$ in size. Spacers of width 3 mm and thickness b are placed along the two long edges of the cell. The two ends of the cell are inserted into plastic blocks. Air is injected through one end and displaces nematic MBBA inside the cell. The displaced nematic flows into a cavity in the plastic block at the other end which is open to air. Details of the construction of the cell and the experimental setup are given in [23].

For $p = 2$ cm Hg, a single finger was observed, with a hump developed as it propagated. For $p = 4$ cm Hg, as shown in figure 5, a series of instabilities developed. The location of the asymmetric tip-splitting and the size of the smaller finger remained unchanged as the faster-growing finger advanced. The length of the farthest tip increased with time t as $t^{1{\cdot}9}$, implying a time-dependent growth rate of $t^{0{\cdot}9}$. This exponent of 1·9 is slightly larger than that of 1·6 observed by Maher [31] in isotropic

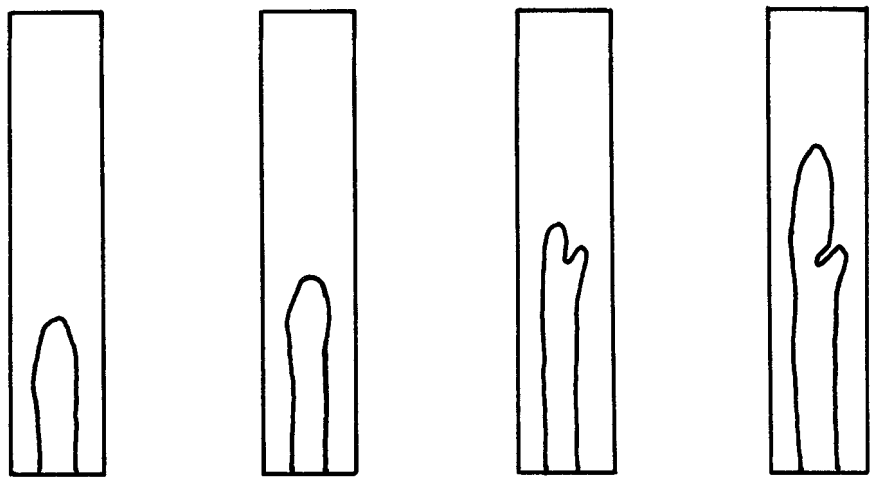

Figure 5. Viscous fingers in linear cell of nematic MBBA. The cell is the same for figures 6–8. $T = 25°C, b = 0{\cdot}3$ mm, $p = 4$ cm Hg. Time increases from (*a*) to (*d*). (*a*) Simple finger. (*b*) Hump. (*c*) Asymmetric tip-splitting. (*d*) One split finger grows while the other remains stable.

liquids during the early state of many fingers coexisting with each other. This larger growth rate is due to the fact that we have a single finger with an essentially constant shape. The exponent is related to the nonstationary state in the experiment and the wetting of the nematic on the glass plates.

For $p = 8$ cm Hg, a time sequence of instabilities was observed in a *single* run of the experiment. The shape of the finger transforms from simple finger to hump, side-wrinkling, tip-splitting and sidebranching (figure 6). In the theoretical study of isotropic liquids, these instabilities were attributed to noise [12–14] while anisotropic surface tension was shown to be essential in producing side-wrinkling [13]. Here, we have a natural medium (nematic) with intrinsic anisotropic surface tension and therefore side-wrinkling is observed.

For 10 cm Hg $\leqslant p \leqslant$ 14 cm Hg, a asymmetric dendrites (figure 7) was observed. The separation between two consecutive bifurcations on one side of the dendrite is found to decrease almost linearly for $p = 10$ cm Hg. For 4 cm Hg $\leqslant p \leqslant$ 14 cm Hg, the width of the first small finger decreases almost linearly with p [23].

For $p = 16$ and 18 cm Hg, sidebranching of the major finger was more dense and DLA-like structure was obtained (figure 8), similar to that predicted by Liang [14]. No dendrites were observed. Therefore, we have a reentrant sequence of tip-splitting, asymmetric dendrite, tip-splitting as a function on p. A similar reentrant sequence was found in a radial cell in [18] as a function of the injected-air flux, except that the dendrites there were more symmetric.

In a thinner cell ($b = 0{\cdot}09$ mm), sidebranching DLA-like structure was observed from the beginning [23]. More detailed results can be found in [23].

For the linear cell the results can be understood qualitatively by (i) the introduction of a time-dependent effective control parameter,

$$1/B_{\text{eff}} \equiv 12(\mu V_n/\sigma)(w/b)^2 \tag{23}$$

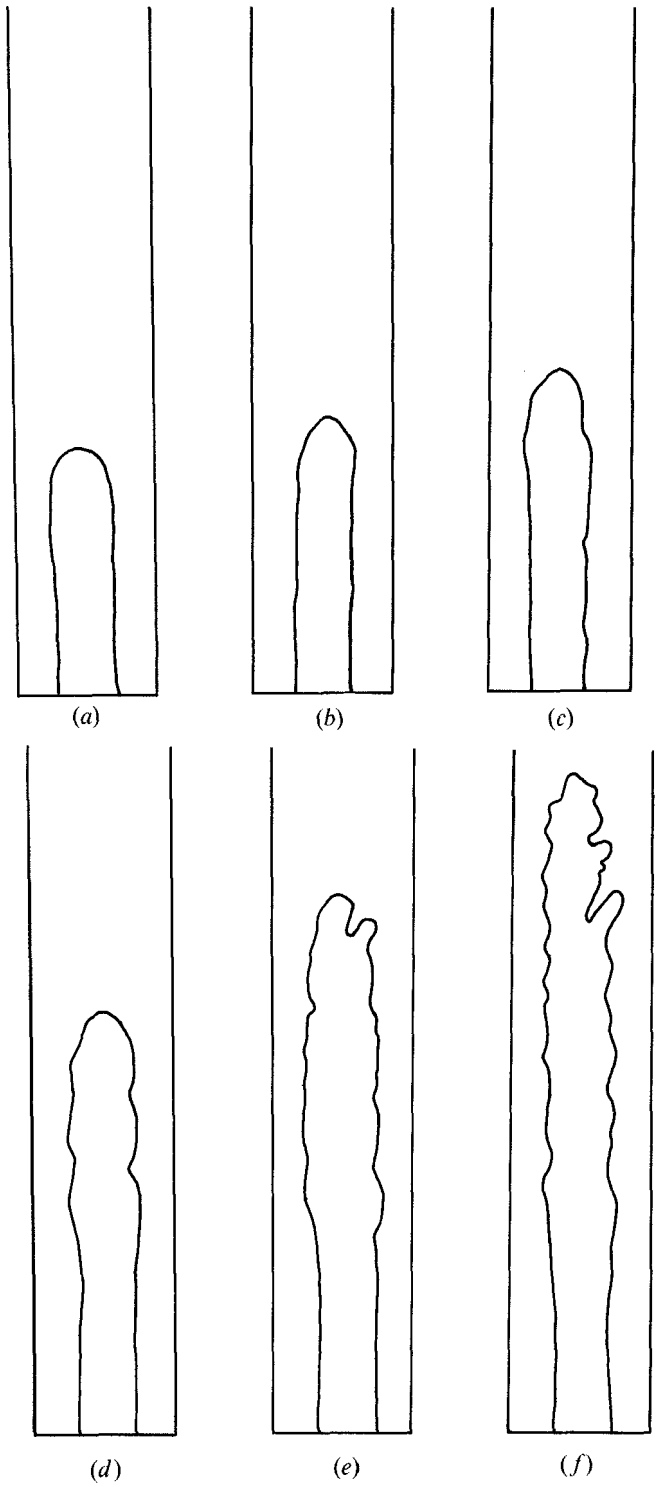

Figure 6. Instabilities of viscous fingers in linear cell. $p = 8$ cm Hg. (*a*) Simple finger. (*b*) Hump. (*c*), (*d*) Side-wrinkling. (e) Tip-splitting. (*f*) Sidebranching. Time increases from (*a*) to (*f*).

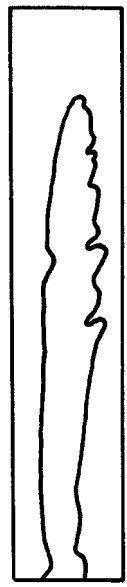

Figure 7. Asymmetric dendritic finger in linear cell. $p = 10$ cm Hg.

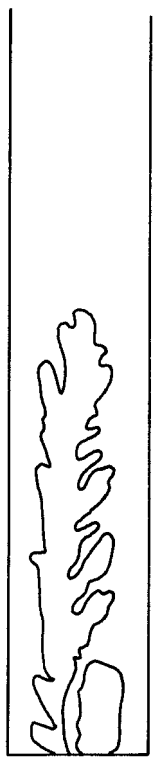

Figure 8. DLA-like structure in linear cell. $p = 16$ cm Hg. The end of the cell is slightly lower than the lower edge shown here.

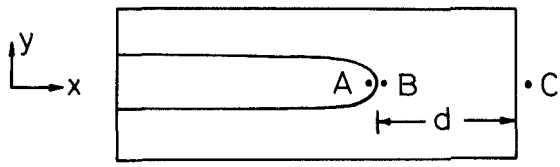

Figure 9. Sketch of a finger in a Hele-Shaw cell.

where V_n is the velocity of the finger tip, and (ii) the assertion that the sequence observed in figure 6 appears as $1/B_{\text{eff}}$ increases. Point (ii) is based on the results in [12, 14]. As shown in figure 9, $V_n \sim \bar{V} \equiv (k/d)(p_B - p_C) = (k/d)(p - \Delta p)$, where $p \equiv p_A - p_C$ and $\Delta p \equiv p_A - p_B$ given by (21). Therefore,

$$V_n \simeq \frac{k}{d}\left\{p - \frac{\pi}{4}\frac{\sigma}{R} - \frac{2\sigma}{b}\left[1 + 3{\cdot}80\left(\frac{\mu V_n}{\sigma}\right)^{2/3}\right]\right\}. \tag{24}$$

Note that Δp is a function of V_n. In general, as the finger tip approaches the end of the cell, V_n, and hence $1/B_{\text{eff}}$, increase with time. By (ii) a sequence of patterns appears. A reentrant sequence will appear if V_n is a nonmonotonic function of p. See [24] for further discussion.

The fact that the fingers are asymmetric in shape and not aligning symmetrically with respect to the central line (the x axis, say) of the cell is a special property of liquid crystals. From (1) and (3), with x and y interchanged, we see that a shear gradient $v_{x,zz}$ can induce a gradient $p_{,y}$, i.e. a shear flow in the x direction will induce pressure difference in the transverse y direction and hence the asymmetries.

For the radial cell with parallel grooves, the effective control parameter, $1/C_{\text{eff}} = 12\mu V_n/\sigma$, is different in the directions parallel and perpendicular to the grooves. The grooves make V_n smaller in the perpendicular direction, resulting in $1/C_\perp < 1/C_\parallel$. Dendrites occur for a larger $1/C$ and hence the result of figure 2(*a*).

4. Conclusion

The advantages of using liquid crystals over isotropic liquids in viscous fingering in Hele-Shaw cells are: (i) All the instabilities predicted for isotropic liquids can also be found in liquid crystals. (ii) Liquid crystal has intrinsic anisotropic properties (such as anisotropic surface tension) which can be finely tuned. They can and sometimes are essential in producing dendritic and side-wrinkling fingers. (*Local* perturbations in the form of a bubble at the finger tip or a very thin thread along the cell can produce dendrites in isotropic liquids [32].) (iii) Unique features of the fingers appear in liquid crystals, such as asymmetric fingers, asymmetric dendrites and reentrant sequence of patterns. (iv) In the case of liquid crystals, more information on the dynamics of the fingers can be obtained from the molecular orientations which can be observed optically using crossed polarizers. This has been used fruitfully in the study of instabilities of moving nematic–isotropic interfaces [33].

It is true that the equations of motion for liquid crystals are more complicated than that for the isotropic liquids. However, as shown in §2, at least in the lowest approximation, this needs not be the case as the relevant equations describing the phenomena are concerned.

In a Hele-Shaw cell, the essence of the approximation of the hydrodynamic equations is dropping $\partial/\partial x$ and $\partial/\partial y$ terms when compared to $\partial/\partial z$ terms, etc.

(see Lamb [25]). The equations obtained in §2 follow from these kinds of approximations and are new, to the best of our knowledge. It should be emphasized that the linearized version is just the first approximation. The next step is to solve the more complicated equations (1)–(7), which is obviously difficult if not impossible. However, the linearized version does point out the similarity (equation (19)) and the difference (equation (20)) with isotropic liquids. It does provide, for the first time, an explanation for the success of Buka *et al.* [19] in the use of isotropic–liquid results in fitting liquid crystal data, even though the linearized version has its obvious limits.

Mechanism involved in tip-splitting, dendrites, sidebranching are discussed extensively for isotropic liquids in [1–17]. In particular, the anisotropy of surface tension, together with noise, have been shown to be essential in producing side-branching [6, 13]. The corresponding cases in liquid crystals are less clear. This has to await the proper development of the equations of motion, and this is exactly the direction we are undertaking in this paper. Our time-dependent 'control parameter' is offered under the quasisteady state assumption. It is useful in the absence of any calculable theory of any real understanding of the mechanisms.

Note that one may generate backflow in a nematic by applying external electric or magnetic fields [34]. Viscous fingering in the presence of backflow remains to be explored. For large air pressure, the air may be able to reverse that part of nematic flowing backward and an asymmetric interfacial profile in the (x, z) plane results. For small p, a thin layer of nematic may actually flow backward, above which the air flows forward.

In the short summary presented in this paper, at this early stage of development of the field, we, as well as others, are just in the process of accumulating experimental data, speculating about the physics, and attempting to build a theory. There remain a large number of interesting and unsolved problems.

References

[1] Bensimon, D., Kadanoff, L. P., Liang, S., Shraiman, B., and Tang, C., 1986, *Rev. mod. Phys.*, **58**, 977.

[2] Saffman, P. G., 1986, *J. Fluid Mech.*, **173**, 73. Homsy, G. M., 1987, *A. Rev. Fluid Mech.*, **19**, 271. Feder, J., 1988, *Fractals* (Plenum).

[3] Witten, T. A., and Sander, L. M., 1983, *Phys. Rev.* B, **27**, 5686.

[4] Sawada, Y., Dougherty, A., and Gollub, J. P., 1986, *Phys. Rev. Lett.*, **56**, 1260. Grier, D., Ben-Jacob, E., Clarke, R., and Sander, L. M., 1986, *Phys. Rev. Lett.*, **56**, 1264.

[5] Langer, L. S., 1980, *Rev. mod. Phys.*, **52**, 1.

[6] Nittmann, J., and Stanley, H. E., 1986, *Nature, Lond.*, **321**, 663. Kertesz, J., and Vicsek, T., 1986, *J. Phys.* A, **19**, L257.

[7] Kessler, D. A., and Levine, H., 1986, *Phys. Rev.* A, **33**, 2621, 2634. Langer, J. S., 1986, *Phys. Rev.* A, **33**, 435. Caroli, B., Caroli, C., Roulet, B., and Langer, J. S., 1986, *Phys. Rev.* A, **33**, 442.

[8] Saffman, P. G., and Taylor, G. I., 1958, *Proc. R. Soc.* A, **245**, 312.

[9] Paterson, L., 1981, *J. Fluid Mech.*, **113**, 513.

[10] Ben-Jacob, E., Deutscher, G., Garik, P., Goldenfeld, N. D., and Lareah, Y., 1986, *Phys. Rev. Lett.*, **57**, 1903.

[11] Degregoria, A. J., and Schwartz, L. W., 1985, *Phys. Fluids*, **28**, 2313.

[12] Bensimon, D., 1986, *Phys. Rev.* A, **33**, 2663.

[13] Li, G., Kessler, D., and Sander, L., 1986, *Phys. Rev.* A, **34**, 3535.

[14] Liang, S., 1986, *Phys. Rev.* A, **33**, 2663.

[15] Park, C. W., and Homsy, G. M., 1985, *Phys. Fluids*, **28**, 1583.

[16] Tabeling, P., Zocchi, G., and Libchaber, A., 1987, *J. Fluid Mech.*, **177**, 67.

[17] (a) BEN-JACOB, E., GODBEY, R., GOLDENFELD, N. D., KOPLIK, J., LEVINE, H., MUELLER, T., and SANDER, L. M., 1985, *Phys. Rev. Lett.*, **55**, 1315. (b) DORSEY, A. T., and MARTIN, O., 1987, *Phys. Rev.* A, **35**, 3989.
[18] BUKA, A., KERTESZ, J., and VICSEK, T., 1986, *Nature, Lond.*, **323**, 424.
[19] BUKA, A., and PALFFY-MUHORAY, P., 1987, *Phys. Rev.* A, **36**, 1527.
[20] BUKA, A., PALFFY-MUHORAY, P., and RACZ, Z., 1987, *Phys. Rev.* A, **36**, 3984.
[21] SHAO, R. F., LIU, H., and LAM, L., 1988, *J. Nanjing Normal Univ.* (*Natural Sci.*), **2**, 59.
[22] ZHENG, S., SHAO, R. F., LAM, L., and SUN, Z. M., 1988, Paper presented at the Centenary Conference of Liquid Crystal Discovery, Beijing, 27 June–1 July 1988, Paper presented at the 12th International Liquid Conference, Freiburg, 15–19 August 1988.
[23] YANG, S. L., LIANG, Z. C., SHAO, R. F., and LAM, L., 1989, in *Wave Phenomena*, edited by Lam, L., and Morris, H. C. (Springer) (Proc. of 1st Woodward Conference, San Jose, 2–3 June, 1988).
[24] LAM, L., 1989, *Wave Phenomena*, edited by L. Lam and H. C. Morris (Springer) (Proc. of 1st Woodward Conference, San Jose, 2–3 June 1988).
[25] LAMB, H., 1932, *Hydrodynamics* (Cambridge University Press).
[26] PARSONS, J. D., 1976, *J. Phys., Paris*, **37**, 1187; 1975, *Molec. Crystals liq. Crystals*, **31**, 79.
[27] STRYLA, B., KUCZYNSKI, W., and MALECKI, J., 1985, *Molec. Crystals liq. Crystals Lett.*, **1**, 33.
[28] PARK, C. W., and HOMSY, G. M., 1984, *J. Fluid Mech.*, **139**, 291.
[29] HORVATH, V., VICSEK, T., and KERTESZ, J., 1987, *Phys. Rev.* A, **35**, 2353.
[30] COUDER, Y., CARDOSO, O., TAVERNIER, P., and THOM, W., 1986, *Europhysics Lett.*, **2**, 437.
[31] MAHER, J. V., 1985, *Phys. Rev. Lett.*, **54**, 1498.
[32] COUDER, Y., GERARD, N., and RABAUD, M., 1986, *Phys. Rev.* A, **34**, 5175.
[33] OSWALD, P., BECHHOEFER, J., and LIBCHABER, A., 1987, *Phys. Rev. Lett.*, **58**, 2318.
[34] BROCHARD, F., PIERANSKY, P., and GUYON, E., 1972, *Phys. Rev. Lett.*, **28**, 1681.